16th World Conference on Earthquake, 16WCEE 2017

Santiago Chile, January 9th to 13th 2017

Paper N° XXXX (Abstract ID)

Registration Code: S-XXXXXXXX

EXPERIMENTALLY VALIDATED ANALYTICAL MODEL OF A SEMI-ACTIVE RESETTABLE TENDON FOR SEISMIC PROTECTION

R. Franco-Anaya[(1)], A. J. Carr[(2)], J. G. Chase[(3)]

[(1)] *Professor, University of Guadalajara, rfrancoanaya@gmail.com*
[(2)] *Emeritus Professor, University of Canterbury, athol.carr@canterbury.ac.nz*
[(3)] *Distinguished Professor, University Canterbury, geoff.chase@canterbury.ac.nz*

Abstract

This paper describes the development of a numerical model to predict the behaviour of a semi-active resettable tendon during seismic testing. Two resettable tendons were installed as lateral bracings in a four-storey one-fifth scale structure to reduce its seismic response. The test structure was subjected to different simulated earthquake ground motions at various peak ground accelerations. Different control configurations for the resettable tendon were used to test the one-fifth scale structure on the shaking table. The analytical model has three primary components: a resettable device, a steel tendon and a steel restraint. Assumptions adopted for the analytical modelling of the semi-active resettable tendon are described. Non-linear dynamic analyses were performed to assess the accuracy of the mathematical model. Displacement time-histories at the third floor of the test structure are used to compare the analytical and experimental results. It is shown that the analytical simulations can closely reproduce the experimentally observed behaviour of the structure.

Keywords: analytical modelling; resettable tendon; semi-active control; energy dissipation; seismic protection.

1. Introduction

Semi-active resettable devices are an emerging technology that improves the response of structures by reducing the earthquake-induced displacements effectively [1, 2]. Resettable energy dissipation devices are fundamentally hydraulic or pneumatic spring elements that possess the ability to release the stored spring energy at any time. Resettable devices behave essentially as nonlinear springs, where the unstressed position can be reset at any time. This resetting releases all the stored energy in the device, resulting in energy dissipation from the structure to which it is attached. The stored energy, that would normally be returned or restored to the structure in the subsequent reversal of motion, is released and hence dissipated from the structural system [2]. Instead of altering the damping directly, the devices nonlinearly alter the structural stiffness. The device offers great reliability due to its reliance on standard hydraulic or pneumatic concepts, particularly when compared with other semi-active control devices that employ more mechanically and dynamically complicated smart materials. Resettable devices rely on very low power consumption and are subjected to a set of decentralised control logic [3, 4].

Analytical predictions are important in the study of the behaviour of structures under severe earthquake ground motions since such large motions could cause catastrophic damage to the structure. Numerical models are essential to understand the nonlinear response of energy dissipation devices and to predict overall structural response. It is equally important to model the behaviour of these devices in order to establish design guidelines and perform comparative studies.

This paper describes the development of a numerical model to predict the behaviour of a four-storey one-fifth scale structure equipped with two semi-active resettable tendons during seismic testing. Shaking table tests were performed on the test structure both with and without semi-active resettable tendons. The resettable tendon, consisting of a resettable device, a steel tendon and a steel restraint, was installed on each side of the structure. The mechanical properties of the devices were modified according to a control algorithm that took into account the measured response of the test structure. Four different earthquake ground motions at various peak ground accelerations were used as input to the shake table. Different control laws were used to manipulate the hysteretic behaviour of the devices during the seismic testing. Assumptions adopted for the analytical modelling of the resettable tendon are described. To compare the analytical and experimental results, displacement time-histories at the third floor of the test structure are utilised. It is shown that the analytical simulations can reproduce the experimentally observed behaviour of the structure closely.

2. Four-Storey Test Structure

To assess the effectiveness of semi-active resettable devices in reducing the seismic response of structures, a series of shaking table tests were performed on the four-storey one-fifth scale structure shown in Fig. 1a. A main feature of this steel moment-resisting frame structure is the incorporation of replaceable fuses located in critical regions of the structure to show the effects of inelastic structural performance under seismic loading [5].

The test structure is a 2.1 m high three-dimensional four-storey frame structure. The frames are built using square hollow steel sections for the beam and column members. The fuses, beam-column joints and other connecting components are made of steel flat bars. Two frames in the longitudinal direction provide the lateral load resistance. Each frame has two bays with 0.7 m and 1.4 m long spans. The short bay is to show earthquake dominated response, while the long bay is to show gravity dominated response by having an extra point load induced by a transversal beam at the mid-span at each level. In the transversal direction, three one-bay frames with 1.2 m long span provide lateral stability and carry most of the gravity load. A one-way floor slab provides a significant proportion of the model mass. The slab is made of steel planks and is connected to a rigid steel plate that acts as a diaphragm. The planks are simply supported on the beams of the transversal frames and on the intermediate beam supported by the long span beams of the longitudinal frames (Fig. 1a).

(a) Test structure

(b) Sytem implementation

Fig. 1 Four-storey test structure and control system implementation

The test structure was designed as a one-fifth scale structure. It was intended to model the structure as a typical four-storey reinforced concrete building, therefore, the natural period of the structure was required to be within 0.4 s to 0.6 s to obtain similar response under earthquake excitation [5]. The equivalent static method, outlined in the New Zealand Loadings Standard NZS 4203: 1993, was employed to calculate the earthquake forces. The seismic weight of the one-fifth scale structure is 35.3 kN. A ductility factor of 6 was adopted for the structural design. Therefore, the test structure was designed for a base shear force of 8.7% of its seismic weight.

3. Semi-Active Resettable Device

In this research, a newly developed semi-active resettable device is proposed to reduce the seismic response of the four-storey test structure [2, 4]. This novel device utilises air as the working fluid for simplicity and can thus make use of the surrounding atmosphere as the fluid reservoir. Fig. 2a shows a photograph of the semi-active resettable device. The device has a two-chambered design that enables the use of each side of the device piston independently (Fig. 2b). This approach treats each piston side as an independent chamber with its own valve and control. Independent chamber design allows a wider variety of control laws to be imposed, because each valve can be operated independently, allowing independent control of the pressure on each side of the piston. The resettable device also offers the opportunity to sculpt or re-shape structural hysteretic behaviour due to the possibility to control the device valve and reset times actively [4, 6].

(a) Resettable device

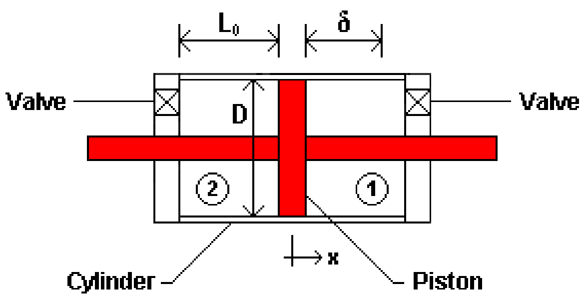

(b) Two-chambered design

Fig. 2 Semi-active resettable device

The piston located inside the cylinder has four seals to ensure minimal air movement between the two chambers, each of the seals is located in a groove. It is important to notice that such air movement would reduce the effective stiffness and energy dissipated by the device. The end caps are press fitted into the cylinder and held in place by eight clamping rods. An O-ring located between the end caps and the cylinder further ensures no leakage of air. Where the piston shaft passes through the end caps, air is prevented from escaping by two seals located in the end caps. Fig. 3a shows a schematic of the semi-active resettable device.

The size of the device and the nominal stiffness required from the device are the principal considerations for the design of the resettable device. Size restrictions may be present during the implementation of the device in structural applications. The device stiffness in turn determines the magnitude of the resisting forces delivered by the device. Additionally, the development of particular forces at specified piston displacements also takes into consideration the size parameters and the stiffness [7]. The fundamental design parameters of the device are the individual chamber length L_0, the maximum piston displacement δ, where $\delta \leq L_0$, and the piston diameter D. The design parameters are shown schematically in Fig. 2b. These parameters can be used to control the stiffness of the device [4, 7].

The nominal device stiffness is dependent on the initial chamber volume and the rate of change of the chamber volume with piston displacement. Both the chamber volume and rate of change of the chamber volume are themselves functions of the device diameter and length, with respect to a given input motion. The semi-active resettable device was designed for a nominal stiffness of 250 kN/m. The device stiffness can be altered by changing the piston design and the chamber length and thus modifying the initial chamber volumes [7]. The resisting force delivered by the device depends on the differential pressure between the two chambers of the device. Therefore, the larger the differential pressure the larger the resisting force produced by the semi-active resettable device.

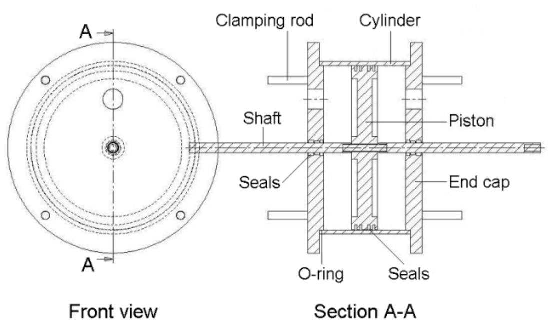

(a) Schematic of the resettable device

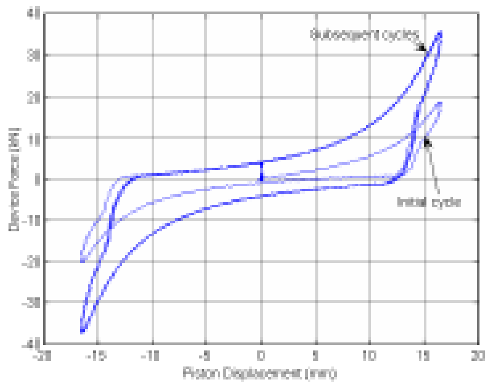

(b) Experimental force-displacement curve

Fig. 3 Schematic of the test device and force-displacement relationship

The dynamic characteristics of the resettable device were identified by experimental tests exploring the response to various input signals. Additionally, the impact and efficacy of different device control laws in adding supplemental damping were investigated. Particular focus was given to the amount of time required to dissipate large amounts of stored energy and its impact on performance, as well as the impact of different control laws on the resulting hysteresis loop. Once the device was characterised, a detailed model was created and validated experimentally [4, 7]. Fig. 3b shows experimental results for the device when subjected to a sine wave input at a frequency of 1 Hz and amplitude of 16.5 mm. The force-displacement curve corresponds to the 1-2-3-4 control law described below. It can be seen that the peak force developed at 16.5 mm displacement is about 35 kN. The frequency of experimental testing is an important factor for practical implementation of resettable devices and should be done at frequencies similar to those expected for earthquake-induced vibrations in structures [6].

4. Implementation of the Control System

Irrespective of the type of device utilised, adding supplemental devices to a frame structure involves increasing the lateral stiffness of the structure. However, a reduction in the lateral stiffness may also be observed when a braced frame structure is replaced by a damper-braced frame structure [8]. An increase in stiffness leads to an increase in the seismic energy input which in turn must be dissipated by the damping devices and/or inelastic action of the structural members. The lateral forces as well as deformations may increase or decrease in the structure, depending on the effect of devices and connections on the dynamic characteristics of the structure, and on the characteristics of the ground motion. Moreover, the magnitude of the increased lateral stiffness in a structure varies depending on the type of device used [8].

The four-storey test structure was tested on a unidirectional shake table. The test structure was bolted to the shake table in such a way that the longitudinal frames of the structure were parallel to the motion of the table. The test structure was tested without the resettable devices (uncontrolled case) and with two resettable devices (controlled case). Different device control laws were used for the controlled case. Each device was installed at the lower end of a steel tendon element. One steel tendon element with a device was installed on each long side of the test structure to remove the potential for any torsional motion. Fig. 1b shows a photograph of the system implementation on the structure. The steel tendon element was placed along the two bays and was connected to the test structure at the third floor to transfer the control forces. This configuration was chosen as a result of an extensive nonlinear finite element investigation of several device architectures [9]. Basically, the semi-actively-controlled tendon connects the seismic centre of mass of the first-mode dominant test structure to the ground.

The dynamic properties of the test structure with and without resettable devices were identified by using free vibration tests. The free vibration tests were carried out by pulling the test structure to one side using a steel wire. After achieving a target floor displacement, the steel wire was cut to allow the structure to vibrate freely. Before attaching the resettable devices to the structure, free vibration testing was carried out with a maximum displacement of 2.5 mm at the top floor to ensure that the test structure remained elastic. The natural period of the test structure was found to be 0.44 s with the corresponding equivalent viscous damping ratio of 1.21% [9].

Four different earthquake ground motions were used as input to the shaking table, namely El Centro 1940 NS, Taft 1952 S21W, Kobe 1995 N000E and Sylmar County 1994. The El Centro and Taft ground motions are historical earthquake records of vibratory nature, while the Kobe and Sylmar earthquakes are recent earthquake records with pulse-type characteristics. The amplitude of the earthquake records was scaled to excite the test structure with earthquake ground motions of different intensity. Some of the records were also modified in such a way that the earthquake velocity did not exceed the maximum velocity (0.24 m/s) of the shake table [10]. The modification of the records ensured that unexpected acceleration spikes did not occur during the testing and that the earthquake records were accurately tracked by the shake table [11].

Various linear potentiometers and accelerometers were used to measure the response of the test structure and the motion of the shaking table. A linear potentiometer located along the axis of each resettable device was used to measure the displacement of the piston shaft with respect to the device housing. The force in each device was measured by a load cell placed between the device and the steel tendon element [9, 11].

5. Control Configurations

As mentioned before, the independent control of the device valves enables the re-shaping of hysteretic behaviour by using different control laws. The control laws are based on the four quadrants defined by a sine-wave motion cycle and they are termed according to the quadrant of the force-displacement relationship in which the device provides resisting forces [4, 6]. Fig. 4 shows the main control laws used in this research. The test structure was tested on the shake table using the following control configurations for the resettable tendon, which includes the resettable device and the steel tendon:

- Valves closed. When the valves of the device are closed, the resettable tendon acts as a rigid bracing system in which the stiffness is provided by the bulk modulus of the air in the device cylinder and the steel tendon.

- 1-2-3-4 control law. The 1-2-3-4 control law provides resisting forces in all four quadrants of the force-displacement curve, as shown in Fig. 4a.
- 1-3 control law. The 1-3 control law is shown in Fig. 4b. This control law provides resisting forces only in the first and third quadrants of the force-displacement graph.
- 2-4 control law. The 2-4 control law provides resisting forces only in the second and fourth quadrants of the force-displacement curve, as shown in Fig. 4c.
- 1-2-3-4 to 2-4 control law. For this particular case, the control configuration is switched from the 1-2-3-4 to the 2-4 control law when the relative displacement across the device exceeds 7 mm in both directions.
- Valves open. By opening the device valves, the resettable tendon serves as a flexible bracing system. When the valves of the device are open, the piston is free to move and the air in the cylinder provides only a small amount of damping due to leakage and heat loss. The friction between the moving parts inside the cylinder also contributes to the damping provided by the device.

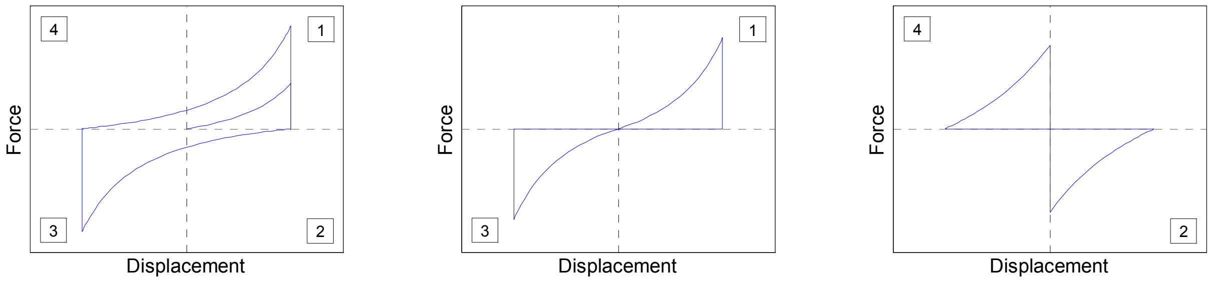

(a) 1-2-3-4 control law (b) 1-3 control law (c) 2-4 control law

Fig. 4 Control laws

The two-chambered design of the test device enables these control laws to be imposed, because each valve can be operated independently which allows the independent control of the pressure on each side of the piston. During the shake table testing, the responses and loads of the test structure were measured and sent to a control computer. The control computer processed the responses according to a predetermined control algorithm and sent an appropriate command signal to the device valves [9, 11].

6. Analytical Model of the Resettable Tendon

A numerical model was developed for application in the RUAUMOKO computer program [12] to simulate the behaviour of the resettable tendon used during the shaking table tests. The analytical model of the resettable tendon is shown schematically in Fig. 5a. The model has three main components. All components are modelled as only carrying forces along the axis of the members. The first component simulates the resettable device (1), the second component represents the steel tendon (2) and the third component models the steel restraint element (3). Each of the nodes of the model has three degrees of freedom. All of the degrees of freedom of the nodes A and D are restrained for fully fixed boundary condition. The horizontal and vertical displacements of the node B are unrestrained however the rotation of the node is restrained. The three degrees of freedom of node C are unrestrained [9].

The semi-active resettable device (1) was modelled by utilising two mechanical springs in parallel. One spring models the hysteretic behaviour of the device and the other spring simulates the friction of the device. The spring member available in the RUAUMOKO program and shown in Fig. 5b is used to represent the resettable device. The computational spring member follows the 1-2-3-4, 1-3 and 2-4 control laws shown in Figs. 4a, 4b and 4c, respectively.

The force developed by the device depends on the pressure of the active chamber and the change in the chamber volume depends on the displacement of the device piston (x). For one change in the chamber volume, the resisting force can be calculated as follows:

$$F(x) = sign(\dot{x})p_0 A\left[\left(\frac{V_1}{V_2}\right)^{\gamma} - 1\right] \tag{1}$$

where γ is the ratio of specific heats, V_1 is the volume of the chamber before the piston displacement, V_2 is the volume of the chamber after the piston displacement, p_0 is the initial pressure (atmospheric), A is the piston area and $\dot{x}$ is the velocity of the device piston.

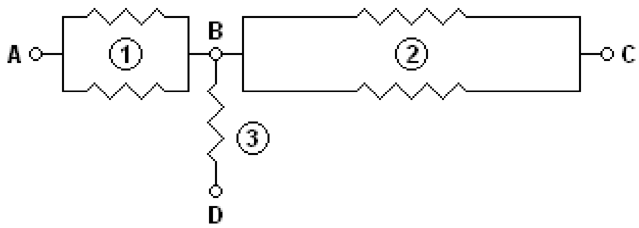

(a) Model of the resettable tendon

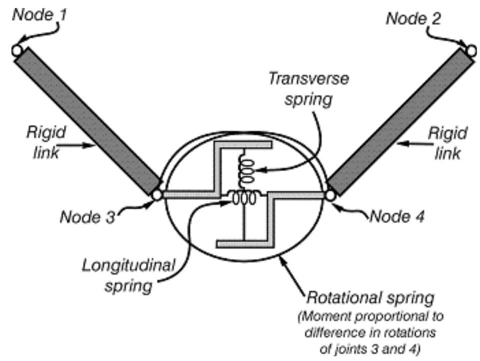

(b) Computational spring member

Fig. 5 Analytical model of the resettable tendon and spring member

For the 1-3 control law, the device force given by Eq. (1) is equal to zero when the displacement and velocity have opposite signs. For the 2-4 control law, the force is equal to zero when the displacement and velocity have the same signs. For all control laws, the device force is set to zero on any change of direction of the displacement. A stiffness of 750 kN/m and a saturation force of 7.295 kN were used to model the hysteretic behaviour of the device. These values were obtained by tuning the model according to the experimental results. The following input data based on actual values of the device and working fluid (air) was used in the computer analyses: p_0 = 100 kN/m^2, γ = 1.4, A = 0.03148 m^2 and L_0 = 18 mm.

A second spring member is utilised to simulate the friction of the device. The spring member follows the elasto-plastic hysteresis rule shown in Fig. 6a. The elasto-plastic spring has a stiffness of 1000 kN/m obtained by fine tuning of the model. A friction force of 430 N based on experimental results [2] was used in the analyses.

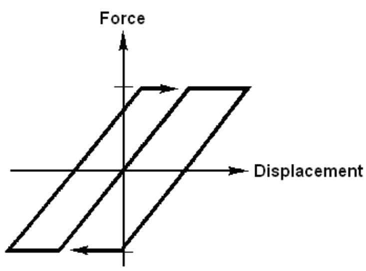

(a) Elasto-plastic

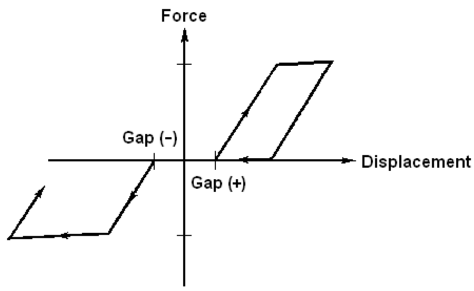

(b) Bi-linear with slackness

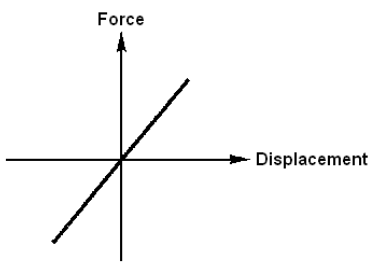

(c) Linear elastic

Fig. 6 Hysteresis rules

The analytical model of the resettable device assumes an ideal behaviour of the device response. This includes the assumptions of instantaneous energy release and exactly symmetrical behaviour. Instantaneous energy release indicates that the response force returns to zero immediately after the device valve is opened. Symmetrical behaviour requires that the centre position of the piston is assigned perfectly.

During the seismic testing, the resettable device was attached to the lower end of a steel tendon (2). The steel tendon was placed along the two bays and was connected to the test structure at the third floor to transfer the control forces. Two mechanical springs placed in parallel are used to model the steel tendon. The assemblage tolerances and slackness of the steel tendon are accounted for by using one of the springs and the second spring is used to stabilise the system. Two spring members are used to model the mechanical springs.

The assemblage tolerances and the slackness of the tendon are modelled by using one of the spring members with the bi-linear with slackness hysteresis shown in Fig. 6b. This hysteresis is used to represent diagonal-braced systems where yield in one direction may stretch the members leading to slackness in the bracing system. The hysteresis allows for either yield in compression in a cross-braced system or for simple elastic buckling in compression which would be more appropriate in a single-braced member [12].

To find the appropriate slackness value (gap length) of the steel tendon was a difficult task. Computer simulations showed that any small variation of the slackness value had a significant impact on the seismic response of the test structure. Besides, the dynamic properties of the structure were affected dramatically. It was observed that a variation of 0.01mm in the slackness value considerably modified the natural frequencies of the structure. A slackness value of 0.2 mm delivered reliable results and therefore was adopted in the analyses.

The other spring member is mainly utilised for numerical stabilization. The stabilization is required to provide control of the node B (Fig. 5a), when the force in the device is zero and the steel tendon is in the gap region shown in Fig. 6b. In this case, none of the components has any stiffness, leading to difficulties in solving the equation of motion at node B. The spring member follows the linear elastic hysteresis shown schematically in Fig. 6c. The actual stiffness of the steel tendon is approximately 35,430 kN/m. In the computer simulations, 90% of this stiffness value was assigned to the spring with gap and 10% was allocated to the elastic spring.

The numerical model of the resettable tendon is completed by a transversal mechanical spring. This spring prevents the movement of the other two components of the model normal to their axes and provides stability to the entire system. An assemblage of steel plates served as the restraint element (3) during the seismic testing. The steel plates were fixed to the shake table to provide support to the resettable device and to suppress any slipping of the device and, consequently, of the steel tendon. The restraint element was modelled by using a spring member with a linear elastic hysteresis (Fig. 6c). Since this elastic spring was required to have a large stiffness, the actual stiffness (180,800 kN/m) of the assemblage of steel plates was utilised in the numerical simulations.

7. Analytical Modelling of Stiff and Flexible Bracing Systems

The mathematical model described in the previous section was also utilised to simulate the behaviour of the rigid and flexible bracing systems during the seismic testing. The stiff bracing system corresponds to the valves closed case in which the resettable device with the valves closed is attached to the steel tendon. The flexible bracing system represents the valves open case in which the resettable device with the valves open is attached to the steel tendon.

When the valves are closed, the resettable device serves as an air spring in which the spring stiffness is provided by the bulk modulus of the air in the device cylinder. For the valves closed case, the test device was modelled using a spring member with a linear elastic hysteresis. A stiffness of 400 kN/m was selected for the linear elastic spring.

When the valves are open, the resettable device provides only a small quantity of damping due to friction, air leakage and heat loss. For the valves open case, the device was also modelled using a spring member with a linear elastic hysteresis. A spring stiffness of 30 kN/m was used for the computer simulations.

It should be noted that the stiffness value of both bracing systems was determined by tuning the analytical model with the results obtained experimentally [9].

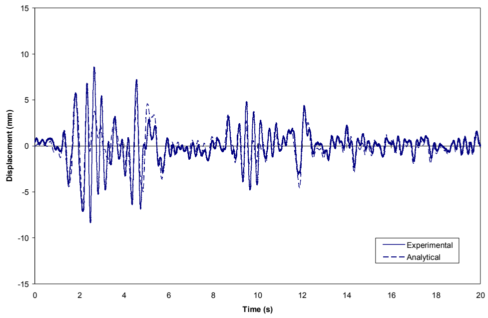

El Centro 60% Earthquake

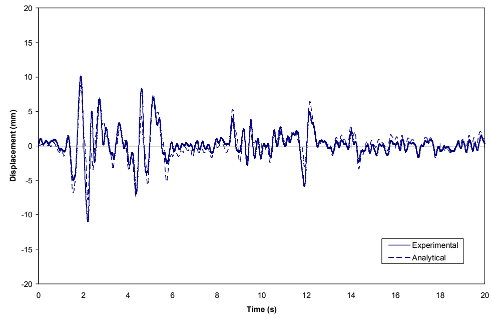

El Centro 60% Earthquake

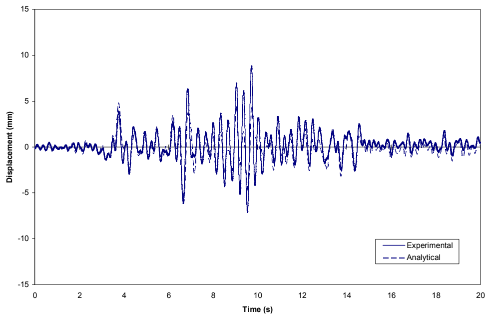

Taft 80% Earthquake

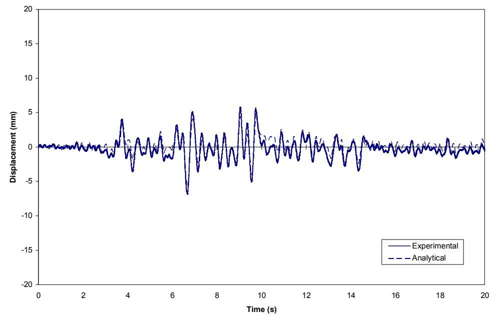

Taft 80% Earthquake

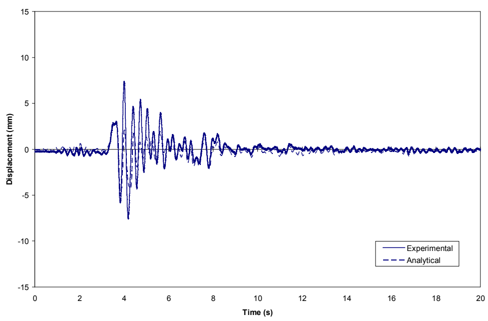

Sylmar 20% Earthquake

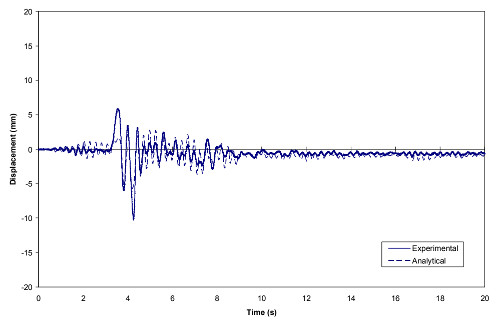

Sylmar 20% Earthquake

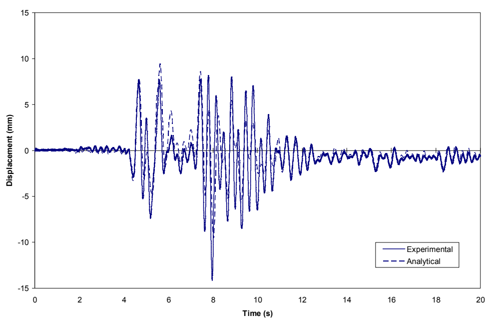

Kobe 25% Earthquake

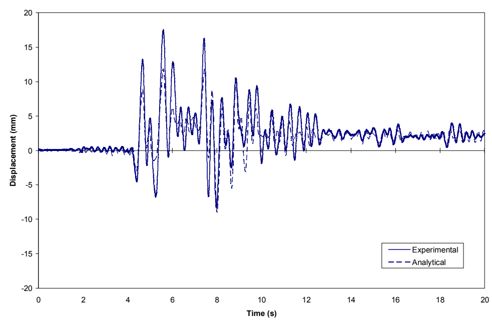

Kobe 25% Earthquake

Fig. 7 Comparison of the displacement time-histories for the 1-2-3-4 and 2-4 control laws

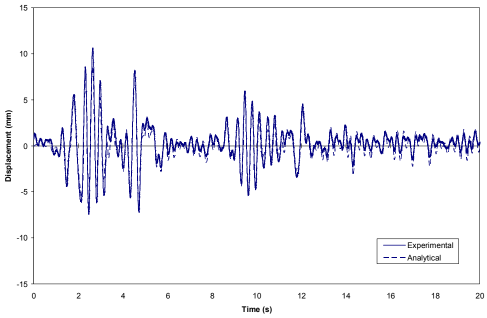

El Centro 60% Earthquake

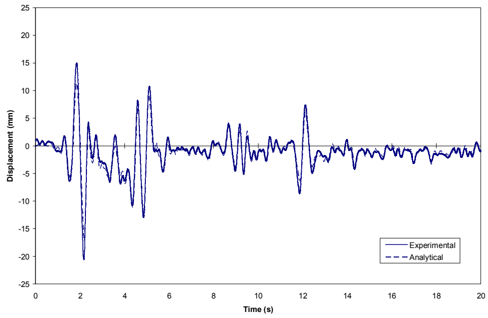

El Centro 60% Earthquake

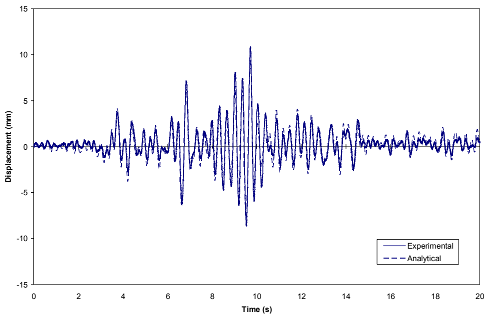

Taft 80% Earthquake

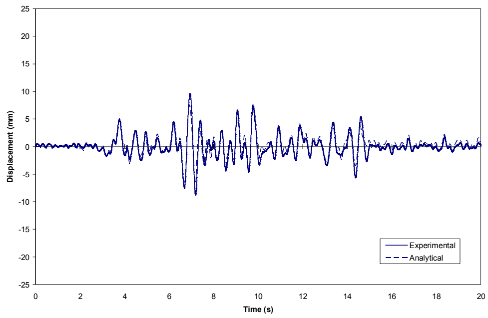

Taft 80% Earthquake

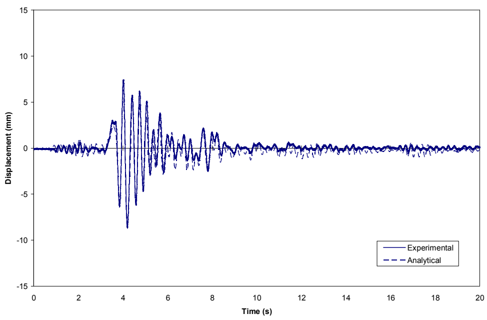

Sylmar 20% Earthquake

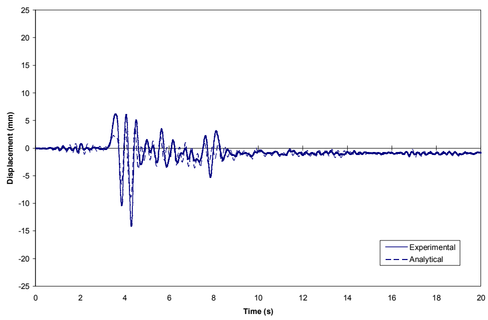

Sylmar 20% Earthquake

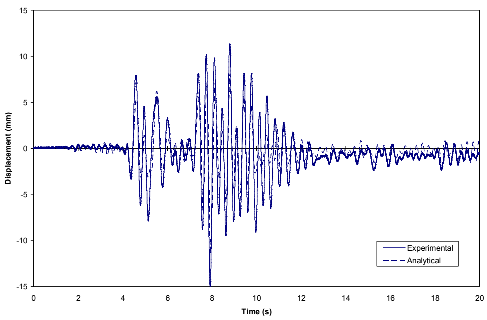

Kobe 25% Earthquake

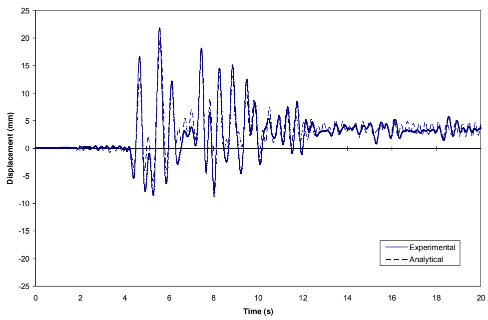

Kobe 25% Earthquake

Fig. 8 Comparison of the displacement time-histories for the valves closed and valves open cases

8. Comparison of Analytical Predictions with Experimental Results

Analytical predictions were obtained by nonlinear computer analyses using the RUAUMOKO program. The numerical model was tuned to the experimental results by using the sub-program HYSTERES available in the RUAUMOKO platform. HYSTERES takes a displacement time-history and computes the associated hysteresis loop for a specified stiffness, yield strength and post-yield behaviour. The sub-program can be used to verify a particular hysteresis loop and to determine the most suitable hysteresis loop for use in a dynamic analysis by selecting the best loop parameters [12].

Fig. 7 and Fig. 8 show comparisons of the results predicted by the numerical model with the results of the shaking table tests. The comparisons are presented in the form of displacement time-histories at the third floor (i.e. the floor that the resettable tendon is attached to). Experimental and analytical results are shown for the 1-2-3-4 and 2-4 control laws, and for the valves closed and valves open cases. The comparisons are presented for selected earthquake ground motions.

Overall, the analytical predictions compare well with the experimental results. It can be seen that the numerical model is able to closely reproduce the main features of the dynamic response of the one-fifth scale structure. In particular, the earthquake response predicted by the numerical model for the 1-2-3-4 control law, and the valves closed and valves open cases is in close agreement with the experimentally observed response.

These results demonstrate that the analytical model developed in this research can be used with confidence to predict and study the behaviour of the test structure under severe earthquake ground motions. However, it is suggested that more research work needs to be done to improve the performance of the analytical model. Future research should include a better representation of the stiffness and friction force of the resettable device. The energy release rate and time, and any response delay of the device valves should be accounted for. Modelling of the slackness of the steel tendon is an important issue that needs improvement. Finally, the impact of the tendon slackness on the earthquake response should be further investigated.

9. Conclusions

An analytical model was developed to simulate the earthquake response of a four-storey one-fifth scale structure equipped with two semi-active resettable tendons. The mathematical model has three primary components. The first component represents a semi-active resettable device, the second component simulates a steel tendon and the third component models a steel restraint element. The three components of the model were modelled using spring members with different hysteretic behaviours. Nonlinear dynamic analyses using the RUAUMOKO computer program were performed to assess the accuracy of the numerical model. Displacement time-histories at the third floor are used to compare the analytical and experimental results. The 1-2-3-4 and 2-4 control laws, and the valves closed and valves open cases are compared for different earthquake ground motions. Comparisons of the analytical predictions with the experimental results indicate that the analytical model is able to simulate the seismic behaviour of the test structure well.

Acknowledgement

This research was a collaborative effort between the Department of Civil and Natural Resources Engineering and the Department of Mechanical Engineering of the University of Canterbury. The first author would like to thank Prof. Athol J. Carr and Prof. J. Geoffrey Chase for their encouragement, guidance and support throughout the research process.

References

[1] Jabbari F, Bobrow JE (2002): Vibration suppression with resettable device. *Journal of Engineering Mechanics*, **128** (9), 916-924.

[2] Mulligan KJ, Chase JG, Mander JB, Rodgers GW, Elliott RB, Franco-Anaya R, Carr AJ (2009): Experimental validation of semi-active resetable actuators in a 1/5th scale test structure. *Earthquake Engineering and Structural Dynamics*, **38** (4), 517-536.

[3] Barroso LR, Chase JG, Hunt S (2003): Resettable smart dampers for multi-level seismic hazard mitigation of steel moment frames. *Journal of Structural Control*, **10** (1), 41-58.

[4] Chase JG, Mulligan KJ, Gue A, Alnot T, Rodgers G, Mander JB, Elliott R, Deam B, Cleeve L, Heaton D (2006): Re-shaping hysteretic behaviour using semi-active resettable device dampers. *Engineering Structures*, **28** (10), 1418-1429.

[5] Kao GC (1998): Design and shaking table tests of a four-storey miniature structure built with replaceable plastic hinges. *M.E. Thesis*, University of Canterbury, Christchurch, New Zealand.

[6] Rodgers GW, Mander JB, Chase JG, Mulligan KJ, Deam BL, Carr A (2007): Re-shaping hysteretic behaviour-Spectral analysis and design equations for semi-active structures. *Earthquake Engineering and Structural Dynamics*, **36** (1), 77-100.

[7] Mulligan KJ, Chase JG, Mander JB, Rodgers GW, Elliott RB (2010): Nonlinear models and validation for resetable device design and enhanced force capacity. *Structural Control and Health Monitoring*, **17** (3), 301-316.

[8] Pekcan G, Mander JB, Chen, SS (2000): Balancing lateral loads using tendon-based supplemental damping system. *Journal of Structural Engineering*, **126** (8), 896-905.

[9] Franco-Anaya R (2008): Seismic performance of semi-active control systems. *Ph.D. Thesis*, University of Canterbury, Christchurch, New Zealand.

[10] Chase JG, Hudson NH, Lin J, Elliot R, Sim A (2005): Nonlinear shake table identification and control for near-field earthquake testing. *Journal of Earthquake Engineering*, **9** (4), 461-482.

[11] Franco-Anaya R, Carr AJ, Chase JG (2014): Shaking table tests of a model structure with semi-active resettable devices. *Proceedings of the 10th National Conference on Earthquake Engineering*, Earthquake Engineering Research Institute, Anchorage, Alaska.

[12] Carr AJ (2006): RUAUMOKO-Inelastic dynamic analysis program. *Computer Program Library*, Department of Civil Engineering, University of Canterbury, Christchurch, New Zealand.